SURF ZONE HYDRODYNAMICS – COMPARISON OF MODELLING AND FIELD DATA

Nicholas Grunnet[1], Kévin Martins[2], Rolf Deigaard[3] and Nils Drønen[4]

Field data from the NOURTEC project is used for comparison with simulation results by the MIKE21 FM model complex. The study includes generation of boundary data by a regional model and simulations by local models of the water level, waves conditions and current fields in the nearshore area of the island of Terschelling.

Keywords: surf zone modelling, field data, waves, tide, current

INTRODUCTION

Numerical models of current and waves are today used in most major coastal engineering projects, but validation studies of complex two-dimensional models for surf zone conditions are rarely found in the literature. This paper presents a numerical modelling study reproducing an extensive series of hydrodynamic field data. The field site is at the central coast of the Dutch barrier island Terschelling, where extensive field measurements were carried out in the spring of 1994 under the NOURTEC project funded by the European Commission's research programme MAST. The numerical models are from the MIKE21 Flexible Mesh suite.

FIELD DATA

The field measurements have been described in detail by Hoekstra et al. (1994) and Grunnet et al. (2004), (2004a) and (2005). A brief outline is given here. The study area is shown in Fig. 1. The main purpose of the NOURTEC experiment was to monitor the development of a 2Mm^3 shoreface nourishment, which was placed in 1993. By the spring of 1994 the nourished sand had been redistributed onshore and welded onto the middle bar. In the following the second of four intensive field campaigns is considered, May-June 1994. The instruments were deployed on a line normal to the coast at station(km) 17. The offshore instruments are placed approximately 5 km from the coastline at 15 m of water depth: A directional wave buoy, P_0, and a tidal station, T1. Meteorological measurements were carried on land.

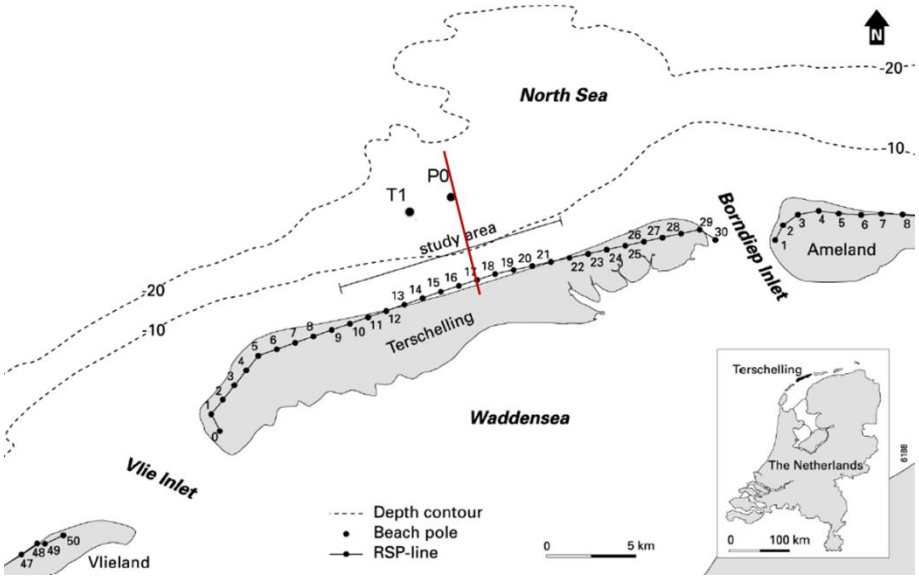

Figure 1. The study site at the island of Terschelling.

[1] DHI France, 4 rue Edouard Nignon, CS 47202, 44372 Nantes Cedex 3, France, ngr@dhigroup.com
[2] DHI France, 4 rue Edouard Nignon, CS 47202, 44372 Nantes Cedex 3, France, Present e-mail address: k.martins@bath.ac.uk
[3] DHI, Agern Allé 5, 2970 Hørsholm, Denmark, rd@dhigroup.com
[4] DHI, Agern Allé 5, 2970 Hørsholm, Denmark, nkd@dhigroup.com

The morphological evolution before and after the field experiment is shown in Fig. 2. The top panel shows the bathymetry before the nourishment. The bathymetry after the nourishment is shown in the second panel, it is seen how the trough inshore of the outer bar has been filled up with nourished sand at stations 14-18. The third panel shows the bathymetry at the time of the campaign, where the trough has been re-established. In the last panel the bathymetry 2½ years after the experiment is shown.

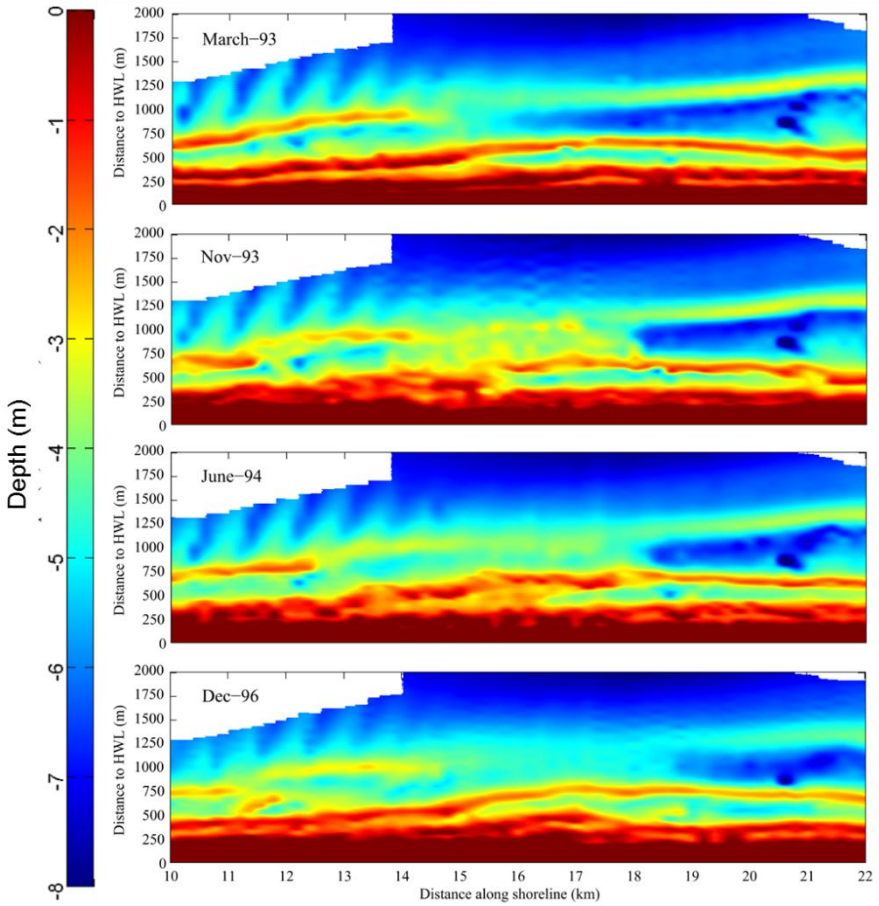

Figure 2. The bathymetry at the site at different times before and after the campaign, depth relative to chart datum.

The locations of the instruments placed in the coastal profile can be seen in Fig. 3. In all six stations a pressure sensor recorded the wave conditions. At four stations, P1, P2, P4 and P5 electromagnetic current meters were also placed, two at each location: 0.25 and 1.2 m from the bed.

The meteomarine conditions, water levels, waves and wind during the campaign are shown in Fig.4.

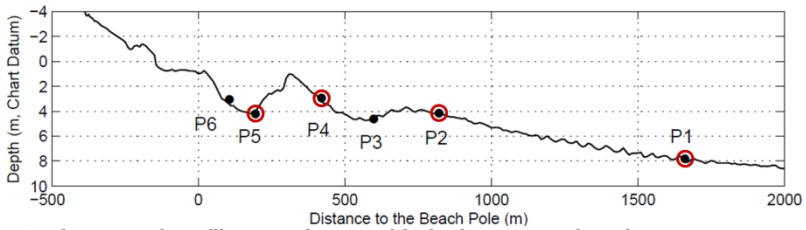

Figure 3. The coastal profile at station 17 with the instrument locations.

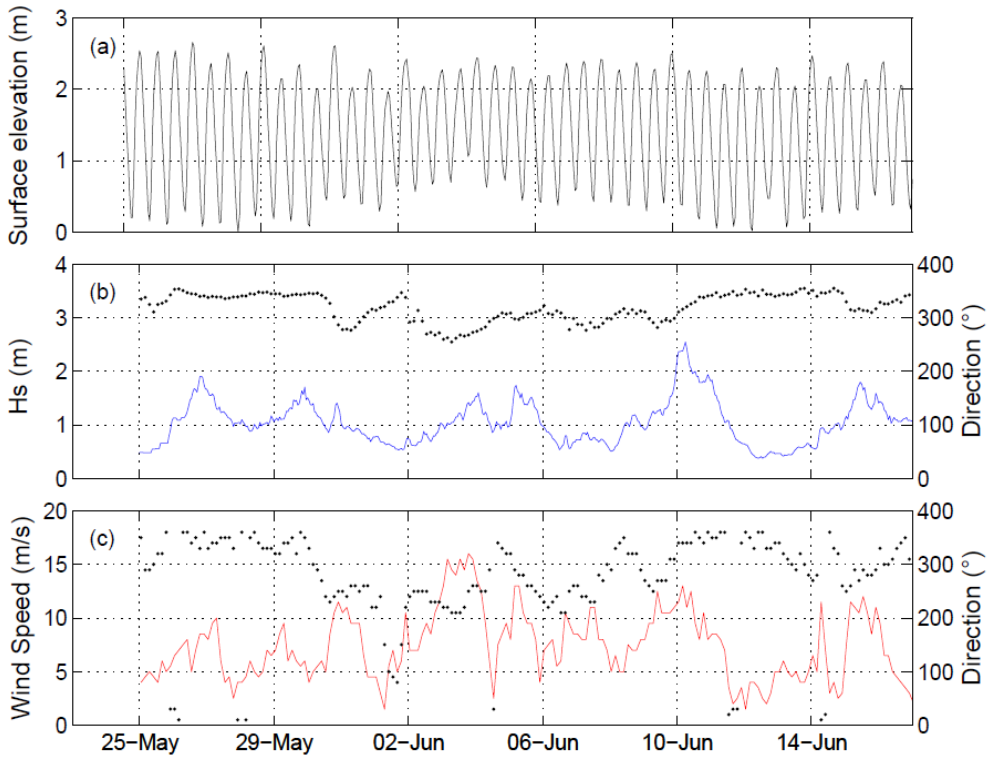

Figure 4. The conditions during the second campaign of the NOURTEC program (May-June 1994). a): water surface elevation relative to chart datum, b): wave conditions, c): wind conditions. Black dots indicate direction of wind/waves.

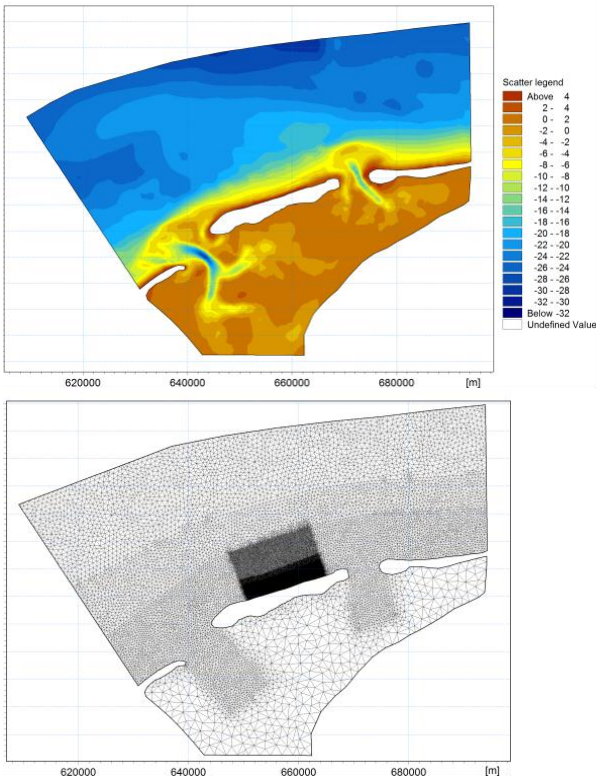

Figure 5. The model domain of the Terschelling model (left) and the computational grid (right).

THE MODELS

The domain of the Terschelling model used for the simulations is shown in Fig. 5. The model has three open offshore boundaries. Inshore of the neighbouring islands the boundaries have been placed at the tidal watershed and treated as closed boundaries together with the land boundaries.

The model grid is also indicated in Fig. 5. The size of the computational cells vary considerably from 500 m^2 in the surf zone in the area of interest, over a few thousand m^2 further offshore in the area of interest to 250-500,000 m^2 in the offshore area. In the Wadden Sea inshore of the islands where the details of the hydrodynamics is of little relevance very large cells up to 2,000,000 m^2 have been used.

Flow model, tide

The flow and wave models are coupled. The hydrodynamics flow model MIKE21 HD calculates the flow field with driving forces from the boundaries, and wind- and wave forcing in the model domain. First the prediction of tide and tidal current is considered. Figure 6 shows the measured and the calculated water levels at station T1. The boundary conditions for the Terschelling hydrodynamic model were water levels obtained from a MIKE 21 North Atlantic Ocean Regional Model, which had proved to be superior to a coarser Global Tide Model. It should be noted that the water levels at station T1 are mainly governed by the boundary conditions and not so much by the local Terschelling Model.

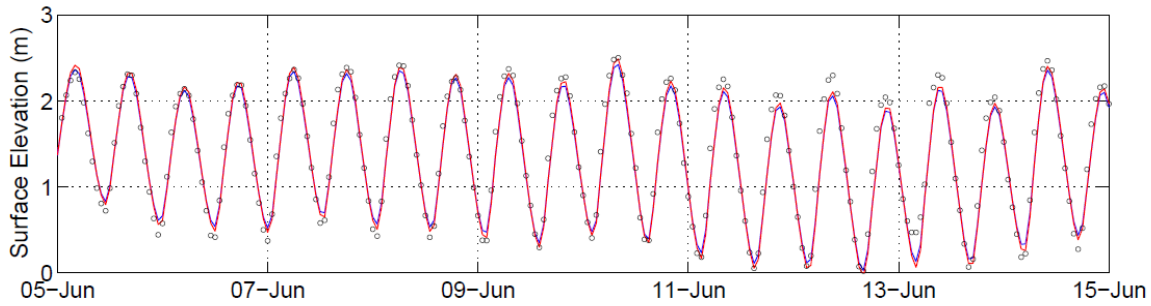

Figure 6. Measured and simulated water levels for June 5-15 1994.

The tidal currents are taken from the period June 12-14, where the wind and the wave forcing were neglegible. Different combination of boundary conditions were tried. Figure 7 shows the simulations with water levels at the boundaries extracted from the regional model. One with varying water levels along all boundaries and one where the the water levels along the east and west offshore boundaries are kept constant equal to the values at the corners with the northern boundary. Logarithmic velocity distributions were assumed when comparing the measured velocities with the depth integrated model results.It is seen that the varying boundary conditions give a better representation of the phase variation across the profile. The agreement is good, with the largest differences at station P5, which is place in the trough behind the most important bar.

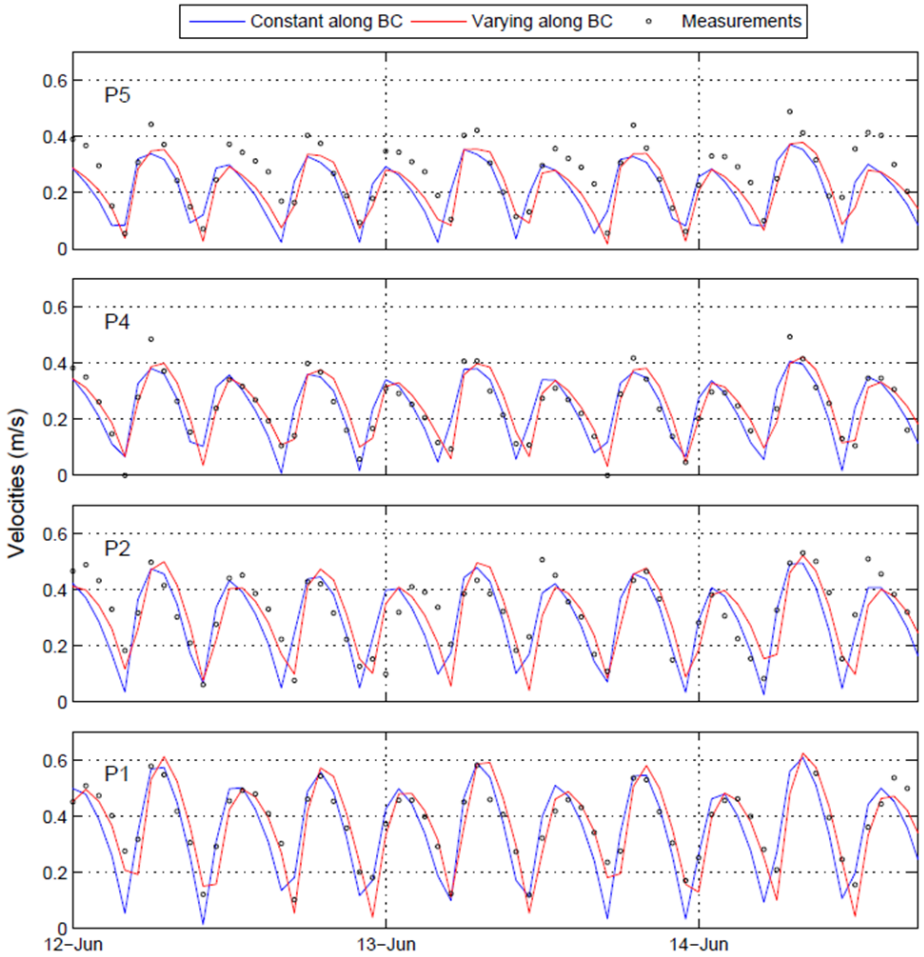

Figure 7. Measured and simulated depth integrated flow speed, June 12-14. Water level boundary conditions for the Terschelling model. Blue curves: constant levels along east and west boundaries. Red curves: varying levels along east and west boundaries.

The current field at flood tide, slack water and ebb tide on May 28, where the wave and wind forcing is weak, is shown in Fig. 8. It is clearly seen how the tidal flow reverses first near the shoreline. This is because the bed friction is strongest here and retards the flow. The nearshore flow with its lower momentum reacts therefore faster to the adverse pressure gradient at slack water. This is similar to wave boundary layers where the flow near the bed reverses earlier than the free stream velocity. Figure 9 shows the three velocity profiles with the flow measurements superposed it is seen that the model clearly captures the measured temporal and spatial variations.

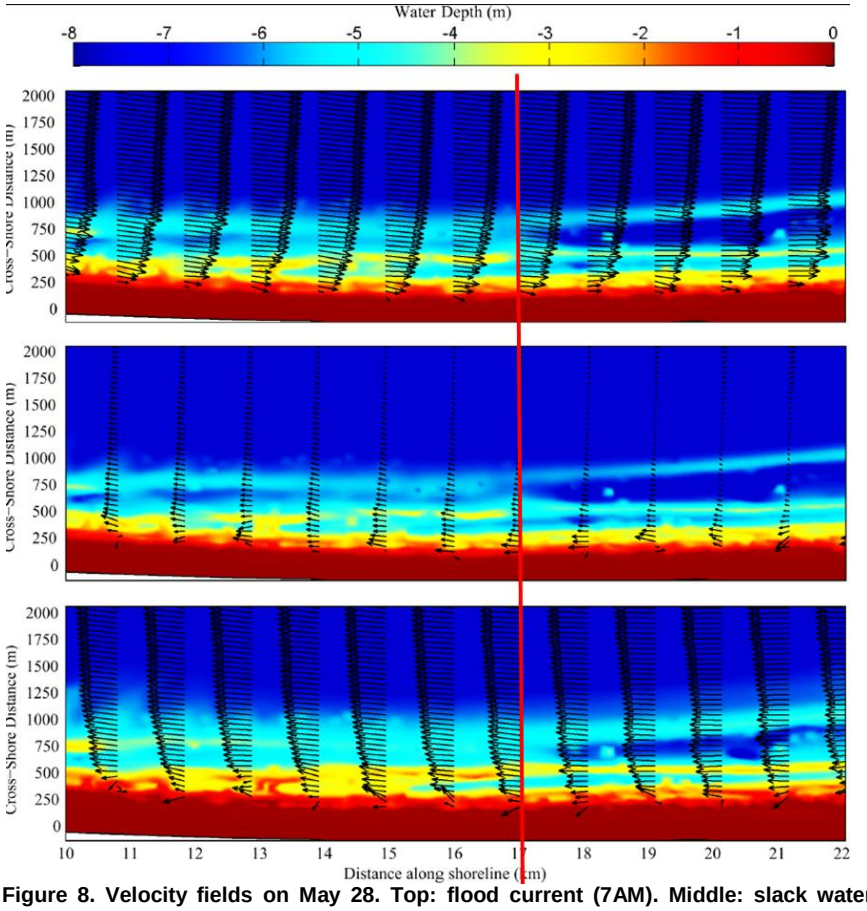

Figure 8. Velocity fields on May 28. Top: flood current (7AM). Middle: slack water (11 AM). Bottom: ebb current (2 PM). Red line indicates position of Station 17 where the instruments were placed.

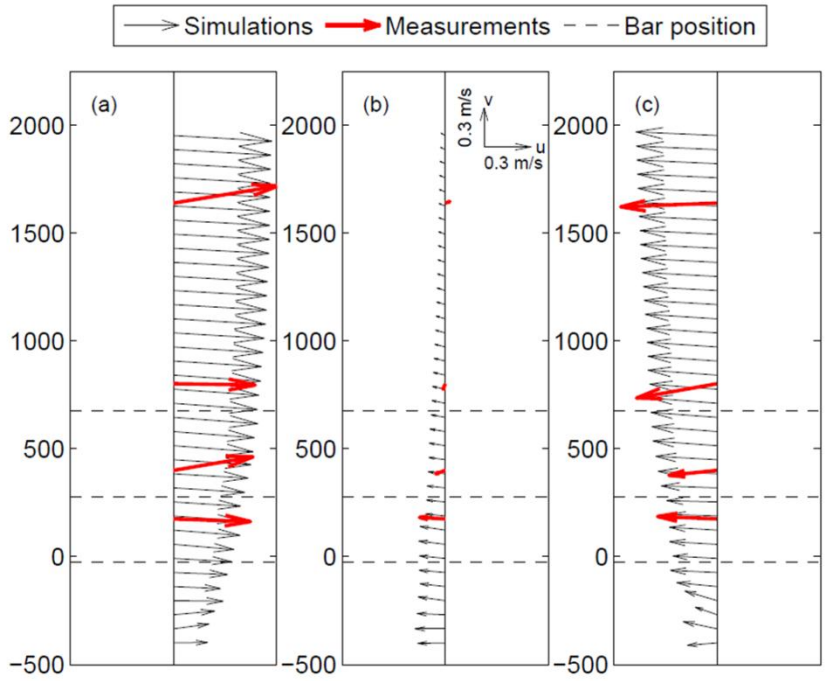

Figure 9. Measured and simulated depth integrated velocities on May 28.

Wave model

The wave conditions were simulated by the spectral MIKE21 SW model. The boundary conditions were obtained from a regional North Sea MIKE21 SW model. Two different forcings, wind and atmospheric pressure, were applied in the regional model. Hourly data from NOAA and an older data set from DMI with 6-hourly values.

Figure 10 shows the measured and the simulated wave heights at Station P1-6. The more recent meteorological data from NOAA give a better prediction of the high waves at the outer station. The effect of wave breaking is clearly seen at the stations closer to the shoreline, in particular in the tidal modulation of the wave height seen from stationP3 and shoreward. The bed roughness, which is important for the dissipation of wave energy by bed friction was used as a calibration parameter. A rather large roughness, up to 6 cm, was applied between station T1 and P1 where ripples were observed, while the roughness offshore was kept at 1.5 cm. Further inshore the wave breaking is the dominant process for wave energy dissipation.

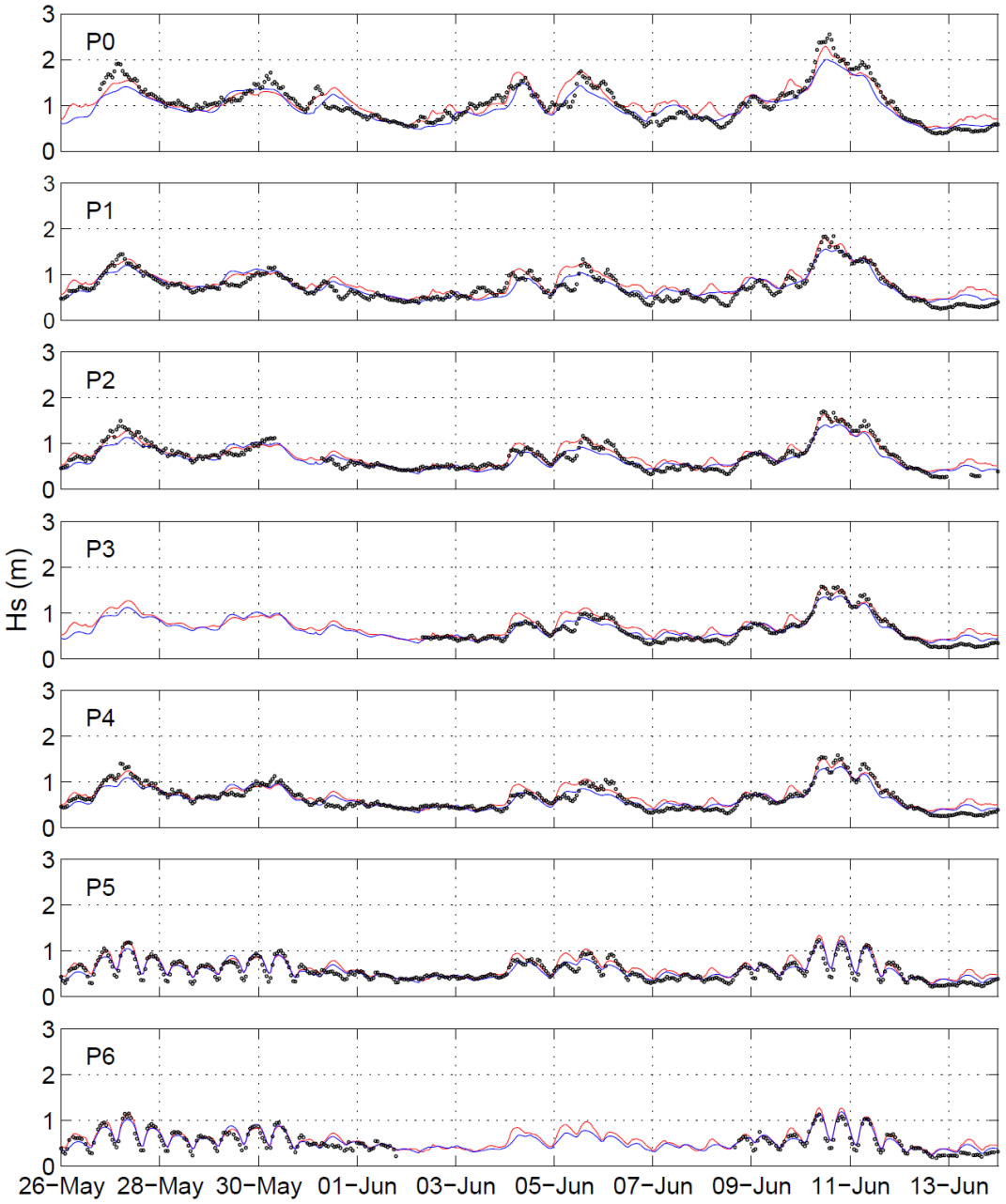

Figure 10. Measured and simulated wave heights. Red curves: using NOAA wind fields. Blue curve using the older DMI model.

The wave breaking in the surf zone is described by the Battjes and Janssen (1978). The variation in wave height across the profile is shown in Fig. 11 for three different stages of the tide. The parameters employed were: alfa = 1.0, gamma1 = 0.7 and gamma2 = 0.88. The concentrated energy dissipation on the bars and the significance of the tide is clearly seen. Different parameter settings were tested including Nelson (1994) and Ruessink (1998). The results did not show high sensitivity to modest changes. The model of Ruessink gave a slight improvement of the prediction for high incoming waves at low tide.

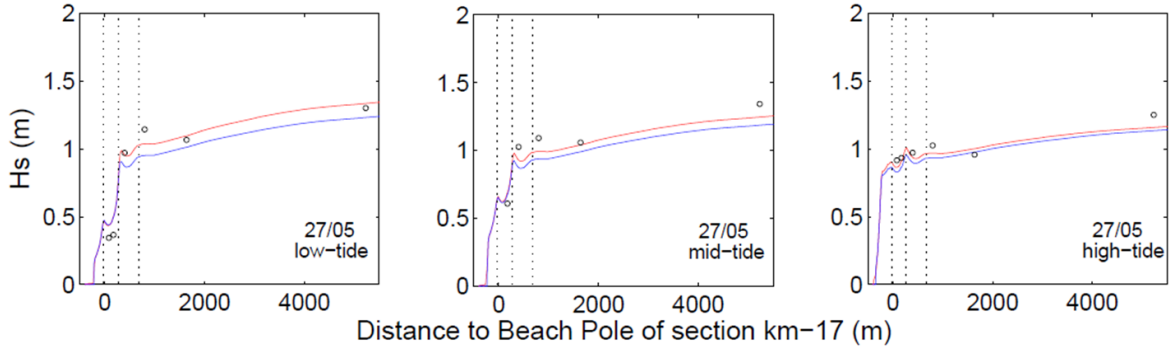

Figure 11. Measured and simulated variation in wave height across the profile at high, intermediate and low tide.

The simulation results shown in Figs. 10 and 11 have been made with parameterized frequency JONSWAP spectra, where the boundary conditions consists of wave height, peak period, mean direction and directional spreading of the wave energy. Simulations with the fully spectral formulation using the complete spectral information at the boundaries gave similar results with respect to the wave parameters predicted by the decoupled parametric formulation, but of course gives more details about the waves conditions, e.g. when combined swell and sea waves were present or with respect to the formation of higher harmonics in the inner surf zone, Fig. 12.

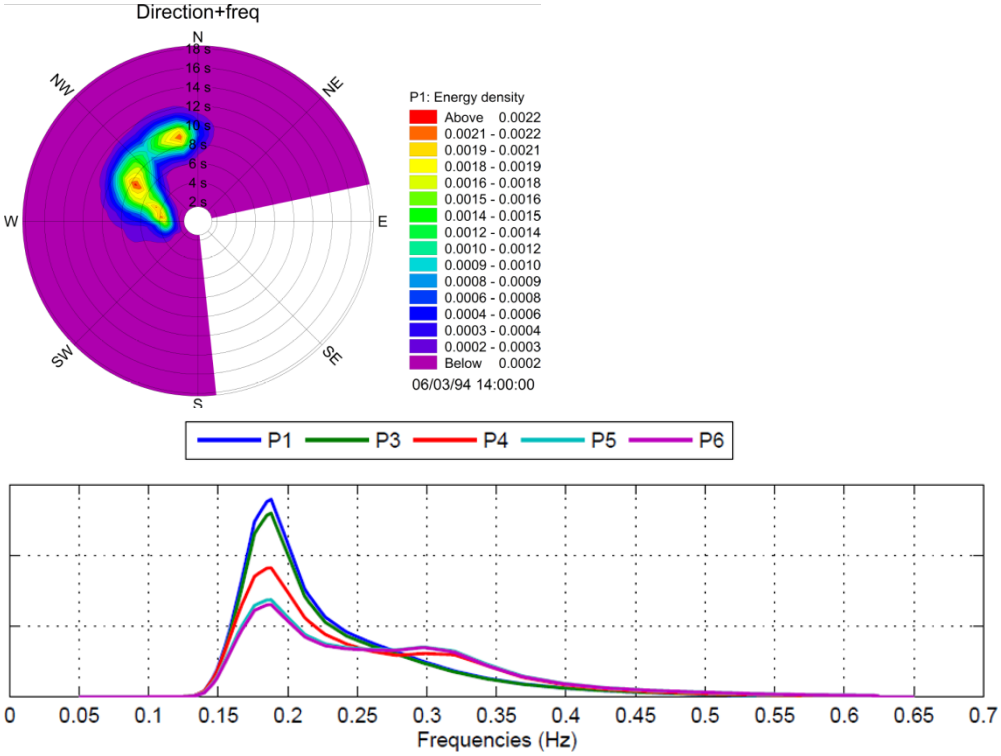

Figure 12. Examples of results from the fully spectral simulation. Top: directional spectrum with wind waves and swell. Bottom: Simultaneous wave spectra at different positions in the profile.

Effect of wind and waves on the current

The forcing from the wind and the waves will affect the current field. This is illustrated in Fig. 13, which shows the measured and simulated current speeds during a period with events with strong winds. Simulation results with forcing from the wind and tide and the tidal current alone is shown. It is seen that the wind forcing becomes dominant on the 3-4th of June where the ebb flow is completely suppressed in the inner part of the profile.

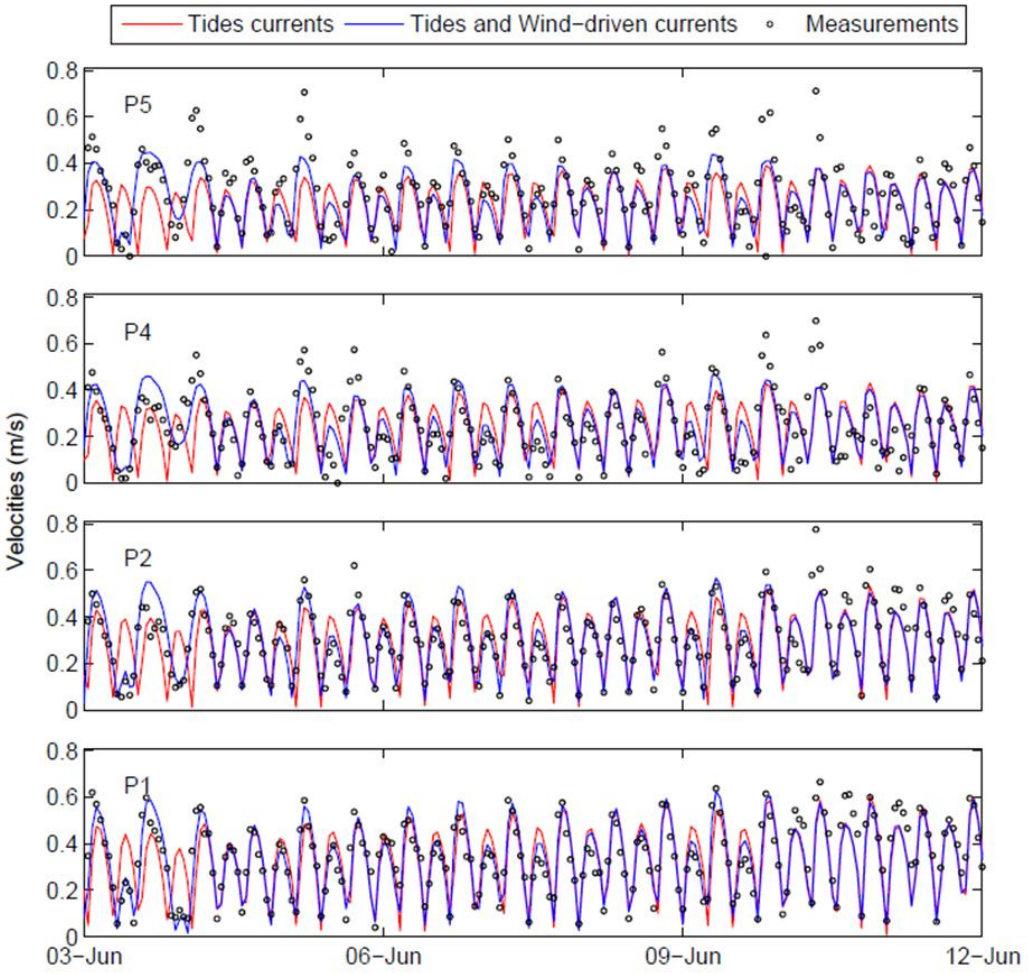

Figure 13. Measured and simulated depth integrated current speed for June 3-12. Red curves: only tidal forcing. Blue curves: forcing from wind and tide included.

Figure 14 show the simulated velocity fields at flood, slack water and ebb. The velocity profiles is presented in Fig. 15 together with the measured velocities. The large difference between the flow driven by wind and tide and the pure tidal flow is seen, and how the latter gives a better representation of the measurements.

The meteorological forcing of the boundary conditions is illustrated by Fig. 16, which shows the water level at station T1 after the tidal signal has been removed. The set-up due to wind and atmospheric pressure is considerably smaller than the tidal range, cf. Fig. 4, and the agreement between the measured and simulated set-up is good.

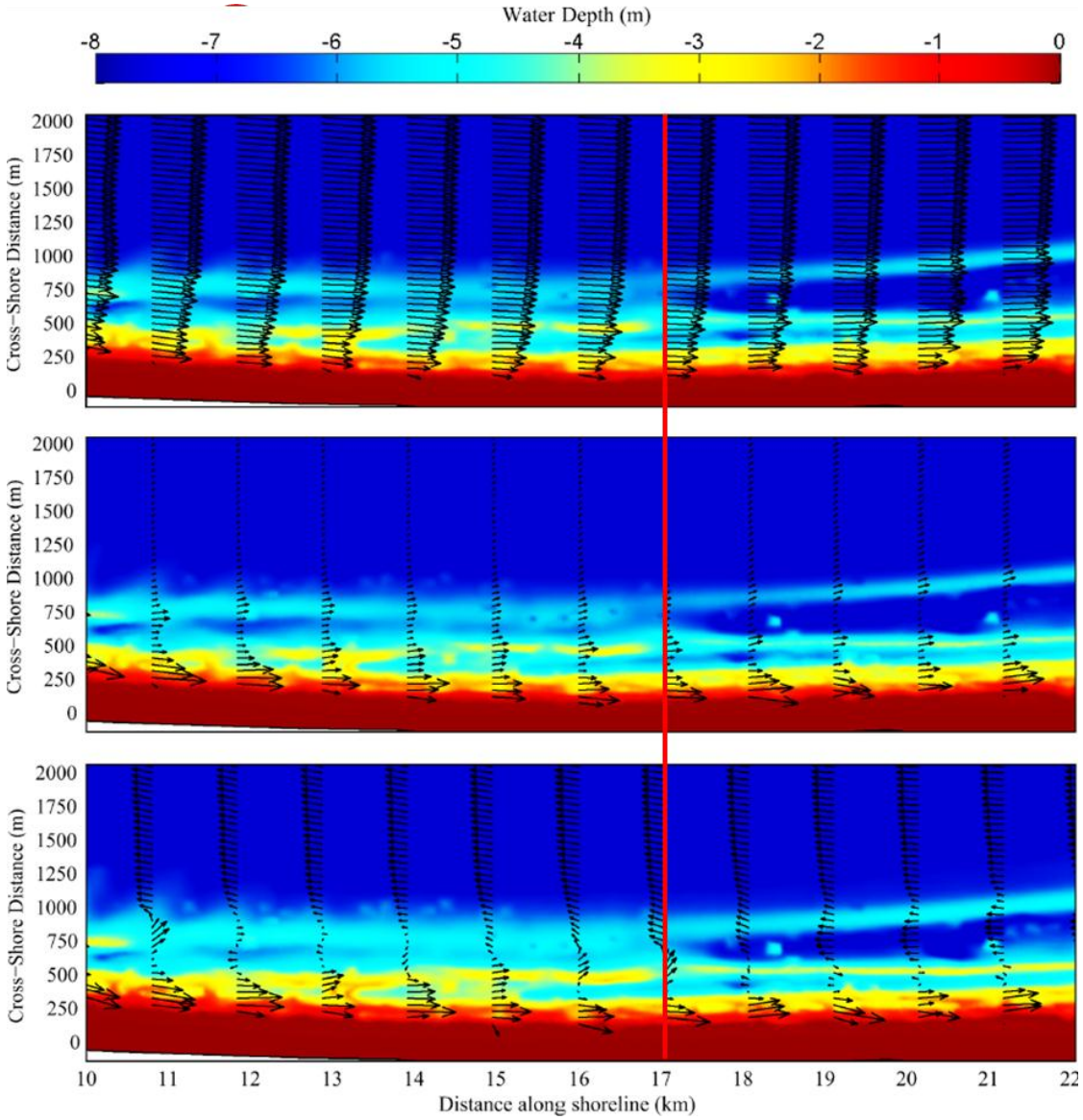

Figure 14. Velocity fields on June 4. Top: flood current (12 AM). Middle: slack water (6 AM). Bottom: ebb current (8 AM).

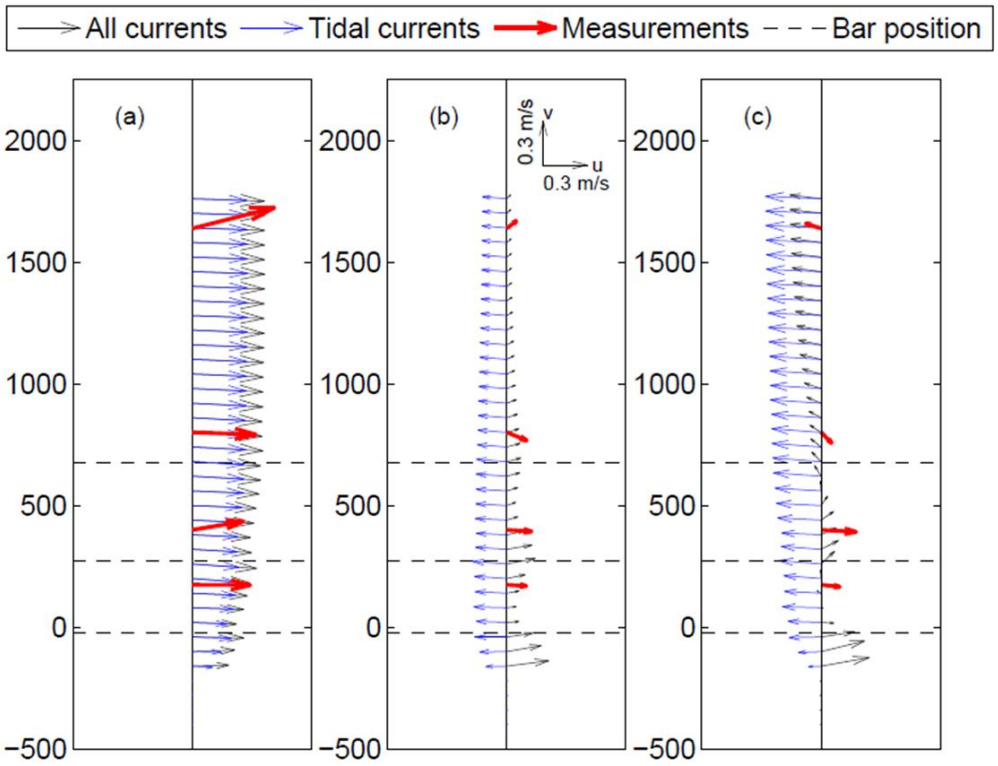

Figure 15. Measured and simulated depth integrated velocities on May 28. Blue arrows: tidal forcing only. Black arrows: forcing by wind and tide.

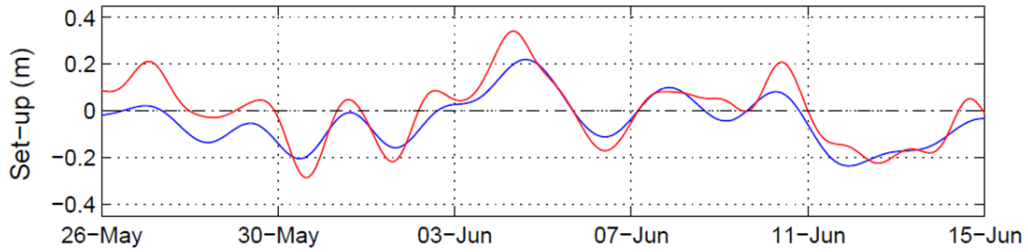

Figure 16. Set-up, water levels with tidal signal removed. Blue curve: measured. Red curve: simulated.

The significance of the radiations stresses from the breaking waves can be seen in Fig. 17, where the simulations with and without driving forces from the waves are depicted. The wave forcing is most important on June 10-11and is most pronounced at station P4, which is located on the outer part of the inner bar. The wave breaking is changing the velocity signal at low water during the ebb current and gives a better agreement with the measurements. The flood currents under high water, where the wave breaking is predicted to be weak, are still under-predicted in this period.

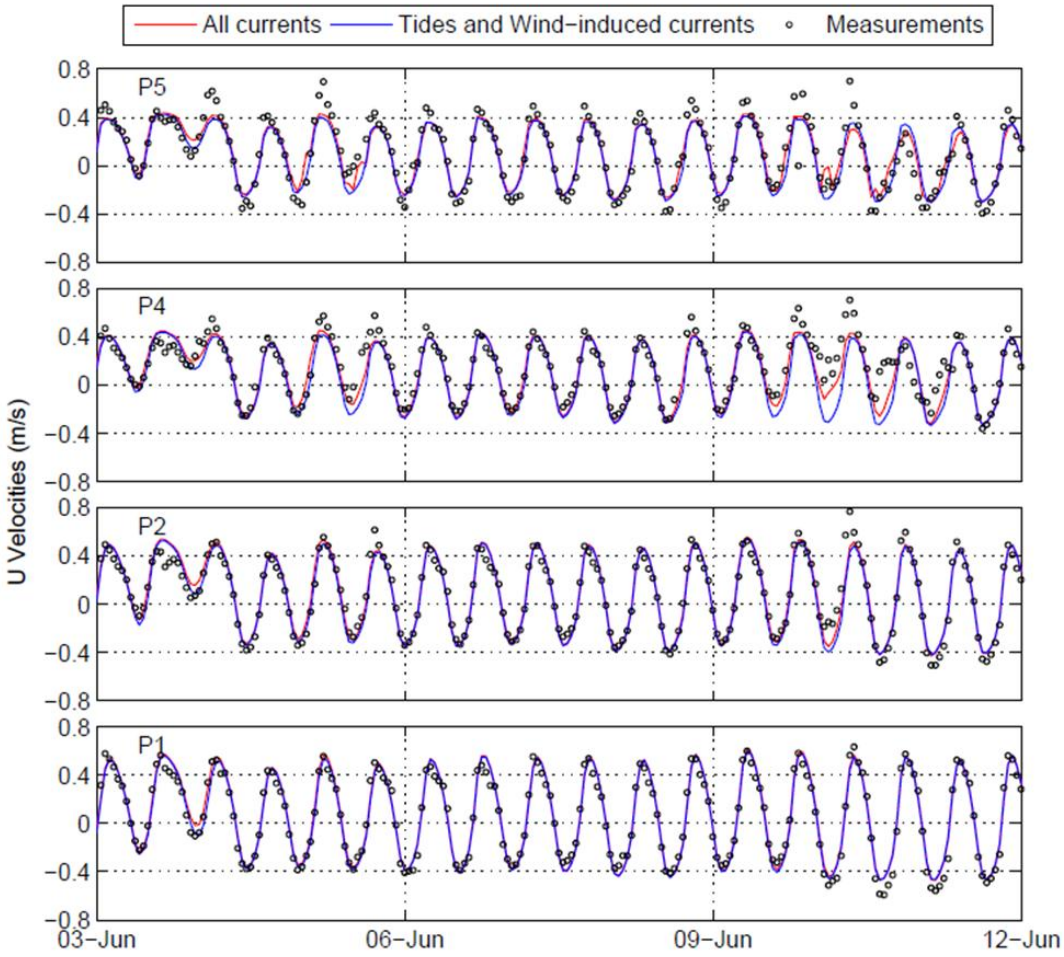

Figure 17. Measured and simulated depth integrated shore parallel current velocities at June 3-12. Blue curves: forcing from wind and tide. Red curves: forcing from wind, tide and waves.

CONCLUSIONS

The hydrodynamic data from the NOURTEC project, which is still one of the best data sets for surf zone conditions, have been used for comparison with simulations made with the flexible grid model MIKE21 FM. The simulations include generation of boundary conditions for the local Terschelling model by regional wave- and current models driven by meteorological and tidal forcing. The Local models simulate the nearshore water levels, wave heights and current fields, which are compared with the field measurements.

ACKNOWLEDGMENTS

The field data from the NOURTEC project have kindly been made available by Prof. Gerben Ruessink, University of Utrecht.

The study has partly been financed by the project: Danish Coasts and Climate Adaptation – flooding risk and coastal protection (COADAPT), financed by the Danish Council for Strategic Research (DFS), project no 09-066869.

REFERENCES

Battjes, J.A., and J.P.F.M. Janssen. 1978. Energy loss and set-up due to breaking of random waves, *Proceedings of 14th International Conference on Coastal Engineering*, ASCE, 466-480.

Grunnet, NM; Hoekstra, P (2004): Alongshore variability of the multiple barred coast of Terschelling, The Netherlands. Marine Geology, Vol.: 203, 1-2, pp.: 23-41.

Grunnet, NM; Ruessink, BG; Walstra, DJR (2005): The influence of tides, wind and waves on the redistribution of nourished sediment at Terschelling, The Netherlands. Coastal Engineering, Vol. 52, 7, pp.: 617-631.

Grunnet, NM; Walstra, DJR; Ruessink, BG (2004a): Process-based modelling of a shoreface nourishment. Coastal Engineering, Vol. 51, 7, pp.: 581-607.

Hoekstra, P; Houwman, KT; Kroon, A; Van Wessem, P; Ruessink, G; (1994): The NOURTEC experiment of Terschelling: process-oriented monitoring of a shoreface nourishment (1993-1994). Proc. 1st int. Conf. on Coastal Dynamics '94, ASCE, New York, pp.: 402-416.

Nelson, R.C., 1994. Depth limited design wave heights in very flat regions. Coastal Engineering Vol. 23, pp.: 43–59.

Ruessink, B.G., 1998. Infragravity waves in a dissipative multiple bar system. Ph.D. thesis. Faculty of geosciences, Utrecht University.